Received March 16, 2019, accepted April 9, 2019, date of publication April 29, 2019, date of current version May 10, 2019.

*Digital Object Identifier 10.1109/ACCESS.2019.2913758*

# Asymmetric Wavelength-Selective Directional Couplers as Fractional-Order Optical Differentiators

**TING-TING YAN, WEN-HUA REN, AND YOU-CHAO JIANG**

Key Laboratory of All Optical Network and Advanced Telecommunication Network, Ministry of Education, Institute of Lightwave Technology, Beijing Jiaotong University, Beijing 100044, China

Corresponding author: Wen-Hua Ren (whren@bjtu.edu.cn)

This work was supported by the Fundamental Research Funds for the Central Universities under Grant 2019JBM012.

**ABSTRACT** In this paper, the asymmetric wavelength-selective directional coupler (DC) is designed as a fractional-order optical differentiator. It is shown that the order of the optical differentiator is determined by the coupling coefficient and the propagation constant difference between the two waveguides in the coupler. The relation between the order of differentiator and the structure parameters of DC is analyzed. Optical differentiators with fractional orders of 0.47, 0.78, and 1.1 based on the asymmetric wavelength-selective DC are designed and analyzed, of which the processing errors are 10.04%, 6.11%, and 22.24%, and the energetic efficiencies are 20.61%, 19.62%, and 20.39%, respectively. The proposed design provides a competitive way for the fractional-order optical differentiator.

**INDEX TERMS** Optical signal processing, pulse shaping, optical devices.

## I. INTRODUCTION

With the rapid development of optical communication, the bit rate of single channel continues to increase. However, in the nodes of optical networks, the transmission signal is processed in the electronic domain, facing many difficulties such as optical-electrical-optical (OEO) bottleneck, large power consumption. All-optical processing, which has advantages of ultra-fast operation speed, small power consumption, has attracted considerable attentions in the past decades [1]–[4].

As a fundamental device of all-optical signal processing circuits, optical temporal differentiator is a device that provides the time derivative of an input optical waveform in optical domain [5]. It can find a wide range of applications such as pulse shaping and coding [6], optical processing and computing [6]–[8], and ultrafast signal generation [6]. The optical temporal differentiators can be classified as integer-order differentiators (IODs) and fractional-order differentiators (FODs). The IODs are proposed firstly and there have been many schemes to implement IODs, such as wavelength-selective DC [5], optical resonator [9], [10], interferometer [11], semiconductor optical amplifier [12], phase-shifted fiber Bragg grating (FBG) [13]–[15], long-period fiber grating [16], [17], phase-modulated fiber Bragg grating (PM-FBG) [18]. The FODs can be regard as a generalization of IODs, which can accomplish what IODs cannot. They have enormous applications because of their distinctive features. One of their features is non-local nature which means that the fractional-order differentiation at a point is not determined by its arbitrarily small neighborhood. For example, Sabatier et al used fractional-order calculus operators to model complex systems with non-local dynamics that have been memorized for a long time [19]. Other distinct features of a fractional differentiator are the ability to distinguish between positive-going and negative-going slopes and the possibility to generate intensity changes from phase variations, which have been used in the space domain, and could be converted to the time domain for signal processing [1], [7]. Currently, the FODs have been implemented with methods such as tilted FBGs [20], [21], electrically tuned silicon-on-isolator Mach-Zehnder interferometer and microring resonator [22], [23], asymmetrical phase-shifted FBGs [24].

In this paper, we proposed an FOD by using the asymmetric DC. Normally, the DC can be made by using the optical fiber or planar waveguide. Compared with DCs based on the planar waveguide, DCs based on the optical fiber have some inherent advantages, such as simplicity, low insertion, and full compatibility with fiber-optic systems. However, they

The associate editor coordinating the review of this manuscript and approving it for publication was Joewono Widjaja.

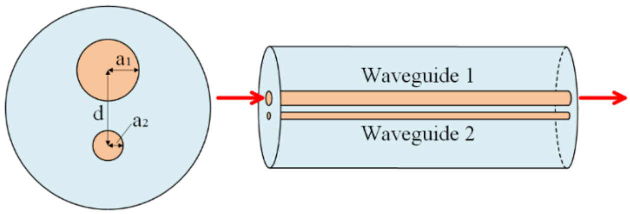


**FIGURE 1.** **The structure diagram of the fractional differentiator based on asymmetrical coupler; $a_1$ and $a_2$ represent the radii of the two waveguides, $d$ represents the core-to-core distance.**

also have shortcomings, such as low level of integration and vulnerability to environmental interference. This paper focuses exclusively on FODs implemented by fiber-based DCs [25].

There are many kinds of methods to make fiber DCs. The fusion-tapering is the most popular method of making fiber couplers. A twin-core fiber, designed to have two cores close to each other throughout its length, can also act as a DC. The model of a twin-core fiber is usually used for theoretical analysis as Fig. 1 shows, where $n_{\text{core1}}$ and $n_{\text{core2}}$ represent the refractive indices of the two waveguides, $n_{\text{clad}}$ represents the refractive index of the cladding.

We will show that when the coupling coefficient and the propagation constant difference of the two waveguides are designed properly, the asymmetric wavelength-selective DCs can work as FODs, which provide a new approach to achieve FODs and have advantages of simple structure and large bandwidth.

The paper is organized as follows. In Section II, the principle of the FODs based on the asymmetric wavelength-selective DCs is presented. In Section III, FODs with different orders based on the asymmetric wavelength-selective DCs are designed. Simulations are carried out to verify the performance of the differentiators, and the results are discussed. A conclusion is drawn in Section IV.

## II. PRINCIPLE

An ideal *n-th* order temporal differentiator is an operator that performs the *n-th* order time derivate of the envelope of an optical signal, whose transfer function can be described as [22], [23], [26]

$$H_n(\omega) = [i(\omega - \omega_0)]^n \tag{1}$$

where $\omega$ and $\omega_0$ are the optical frequency and the carrier frequency, $n$ is the differentiation order, $i$ is the imaginary unit. From the Eq. (1), it can be known that an ideal $n$-th order temporal differentiator can be achieved by using an optical filter that has a magnitude response of $|\omega - \omega_0|^n$ and a phase shift of $n\pi$ at $\omega_0$.

For an asymmetric directional coupler, spectral transfer functions are [5]

$$H_1(L) = \cos(k_e L) + i(\delta_a/k_e)\sin(k_e L) \tag{2}$$

$$H_2(L) = (ik_{21}/k_e)\sin(keL) \tag{3}$$

where $\kappa_e = \sqrt{\kappa^2 + \delta_a^2}$, $\kappa = \sqrt{\kappa_{12}\kappa_{21}}$, $\delta_a = (\beta_1 - \beta_2)/2$, $\kappa_{12}$ and $\kappa_{21}$ are the coupling coefficient (coupling strength per unit length), $\beta_1$ and $\beta_2$ are the propagation constants of the waveguide 1 and 2 of the coupler, $L$ is the length of the coupler. The coupling coefficient between the two waveguides can be calculated [27]

$$\kappa_{pq} = \frac{\omega\varepsilon_0 \int_{-\infty}^{\infty}\int_{-\infty}^{\infty}(N^2 - N_q^2)E_p^* E_q dxdy}{\int_{-\infty}^{\infty}\int_{-\infty}^{\infty}(E_p^* \times H_q + E_p \times H_p^*)dxdy} \tag{4}$$

Here, $E_{p/q}$, $H_{p/q}$ are the electric field and magnetic field distribution of the fundamental mode of waveguide $p$, $q$ respectively. The actual value of $(N^2 - N_q^2)$ in waveguide $p$ equals $(n_{corep}^2 - n_{clad}^2)$ and zero in the rest of regions. According to the calculation results, the coupling coefficient depends on the parameters of the two waveguides, i.e., the refractive indices, the radii and the core-to-core distance of two waveguides.

In previous studies, the symmetric and asymmetric DCs were designed as IODs (1st-order or 2nd-order). For the symmetric DC, it can be designed as IOD when considering that the coupling coefficient of the DC depends on the frequency while the propagation constant difference of the two waveguides doesn't vary along with frequency and keeps at zero [28], [29]. For the asymmetric DC, it can be used as IOD when considering that the propagation constant difference of the two waveguides depends on the frequency while the coupling coefficient of the coupler is a constant [5], [30], [31]. However, for a practical asymmetric DC, both the propagation constant difference $\delta_a$ and coupling coefficient $\kappa$ changed with the frequency, as seen in Fig. 2.

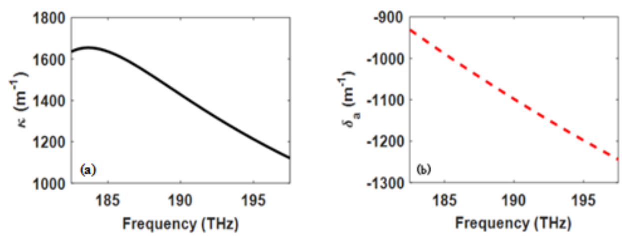


**FIGURE 2.** **The coupling coefficient and propagation constant difference of the asymmetric DC with $a_1 = 3.25$ $\mu m$, $a_2 = 3.5$ $\mu m$, $d = 9$ $\mu m$, $n_{\text{core1}} = 1.449$, $n_{\text{core2}} = 1.449$, $n_{\text{clad}} = 1.444$.**

Considering the frequency dependency of both the coupling coefficient and the propagation constant difference, the magnitude response and the phase response of an asymmetric DC derived from (2) can be expressed as

$$|H_1 L|^2 = cos^2(\kappa_e L) + [\delta_a/\kappa_e sin(\kappa_e L)]^2 \tag{5}$$

$$\Phi = \begin{cases} arctan\{\delta_a sin(\kappa_e L)/[\kappa_e cos(\kappa_e L)]\} & \omega < \omega_0, \\ arctan\{\delta_a sin(\kappa_e L)/[\kappa_e \cos(\kappa_e L)]\} + 2m\pi & \omega > \omega_0, \quad m = 0, 1 \end{cases} \tag{6}$$

When $\kappa_e L = 2m\pi + \pi/2$, with $m = 0, 1, 2, 3, \ldots$, the Eq. (5) reaches its minimum at the central frequency. In this case, the magnitude response of the system function is concave in the neighborhood range of the central frequency, which is similar to the shape of the ideal differentiator.

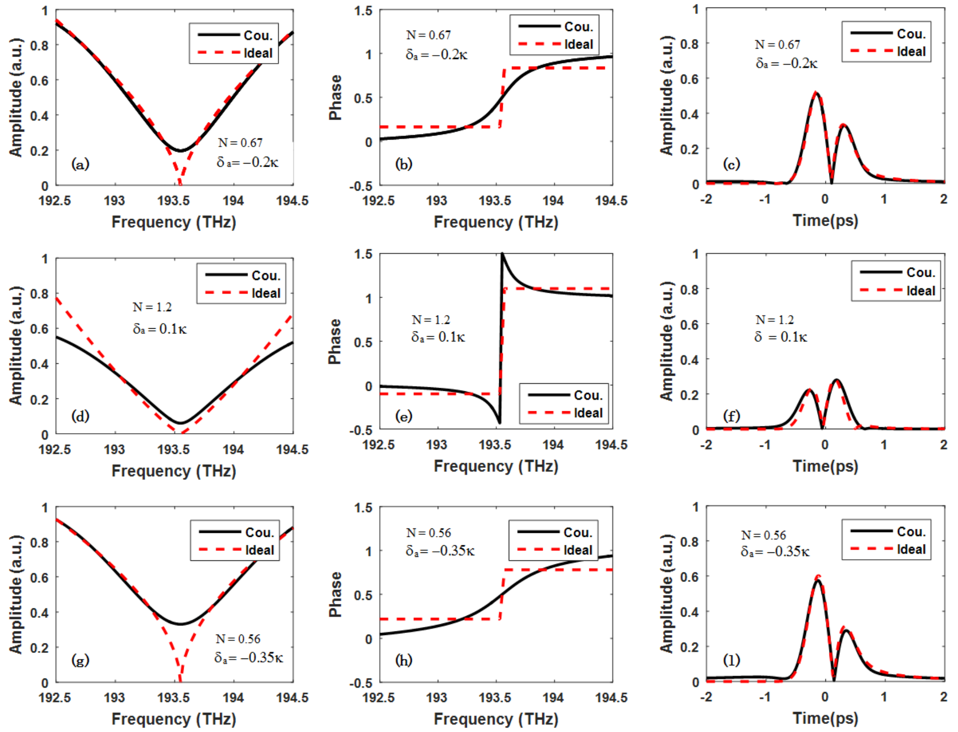

**FIGURE 3.** (a) (d) (g) The magnitude response of the transmission spectrum. (b) (e) (h) The phase response of the transmission spectrum. (c) (f) (i) Output pulse when inputting a Gaussian pulse. Black lines represent the asymmetric DC, and red lines represent the ideal FOD.

Based on the above analysis that both the $\delta_a$ and $\kappa$ depend on frequency, we assume three sets of parameters that $\delta_a = -0.2\kappa$, $\delta_a = 0.1\kappa$, $\delta_a = -0.35\kappa$ with $n_{\text{core1}} = 1.449$, $n_{\text{core2}} = 1.449$, $n_{\text{clad}} = 1.444$. Then, the magnitude and phase responses obtained from (5) and (6) are shown in Fig. 3(a, d, g) and Fig. 3(b, e, h). By comparison with the ideal amplitude responses and ideal phase responses, we can find that these responses just satisfy the responses of the ideal FODs with $N = 0.67, 1.2, 0.56$, where $N$ means the order of FOD. When a Gaussian pulse with a temporal full width at half-maximum (FWHM) of 0.33 ps is input into $a_1$, the output pulses from $a_1$ are shown in Fig. 3(c, f, l). The output waveform from the asymmetric wavelength-selective DC is nearly consistent with that from the ideal FOD. Hence, the FOD can be achieved by using asymmetric wavelength-selective DC if we can find a specific structure i.e., proper parameters of the DC.

## III. DESIGN AND DISCUSSION

In order to achieve the proposed FOD, the parameters of the asymmetric wavelength-selective DC should be designed properly. There are six parameters $a_1$, $a_2$, $d$, $n_{\text{core1}}$, $n_{\text{core2}}$, $n_{\text{clad}}$. For simplifying the problem, we only control $a_1$, $a_2$ to change the coupling coefficient and the propagation constant difference with $d = 9\ \mu m$, $n_{\text{core1}} = 1.449$, $n_{\text{core2}} = 1.449$, $n_{\text{clad}} = 1.444$.

Firstly, a Gaussian pulse is input into waveguide 1 as the input pulse and an output waveform can be obtained from waveguide 1. Different processing errors are calculated by comparing the output waveform that comes from the DC and different ideal output waveforms that come from different ideal FODs. If the minimum of processing error can meet the limitation, it's supposed that the asymmetric DC can be used for FOD. The order of the FOD is the same as the order of the ideal FOD when the processing error is smallest. Otherwise, it's supposed that the asymmetric DC can't be used for FOD.

Through the analysis of a large number of asymmetric DCs with specific structures, a part of asymmetric DCs are appropriate for making the FODs. For example, we set $a_1 = 3.6\ \mu m$, $a_2 = 3.7\ \mu m$ and the magnitude and phase responses are shown in Fig. 4(a, b). Then we compare the output wave-forms with ideal waveforms that obtained from different $n$-th order ideal FODs, and the order of the proposed FOD can be defined as 0.47. The output waveform is shown in Fig. 4(c) and it can be seen that the waveform agrees well with the ideal waveform. Similarly, the FODs with orders of 0.78 and 1.1 can be achieved as Fig. 5 and Fig. 6 show. We find that when the propagation constant of the waveguide 1 is larger than that of waveguide 2, the order of the proposed FOD is larger than 1, otherwise, the order is less than 1.

In all cases, power transfer to the second core occurs in a periodic fashion. The maximum power is transferred at distances such that $\kappa_e z = m\pi/2$, where $m$ is an integer. The shortest distance at which maximum power is transferred to the second core for the first time is called the coupling length and is given by $L_c = \pi/(2\kappa_e)$. The coupling lengths

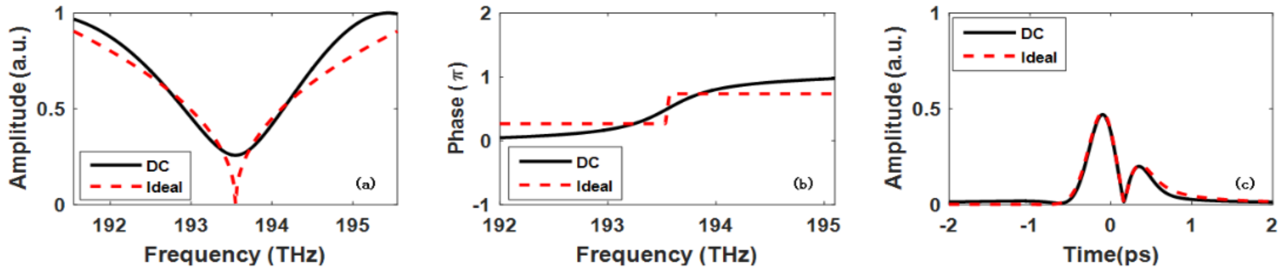


**FIGURE 4.** (a) Magnitude response and (b) phase response of the transmission spectrum of the asymmetric DCs with $a_1 = 3.6\ \mu m$, $a_2 = 3.7\ \mu m$, $d = 9\ \mu m$, $n_{core1} = 1.449$, $n_{core2} = 1.449$, $n_{clad} = 1.444$. The dashed line shows the magnitude and phase response of an ideal FOD. (c) Simulated output pulse. The dashed line shows the output pulse from an ideal FOD. The fractional order is 0.47.

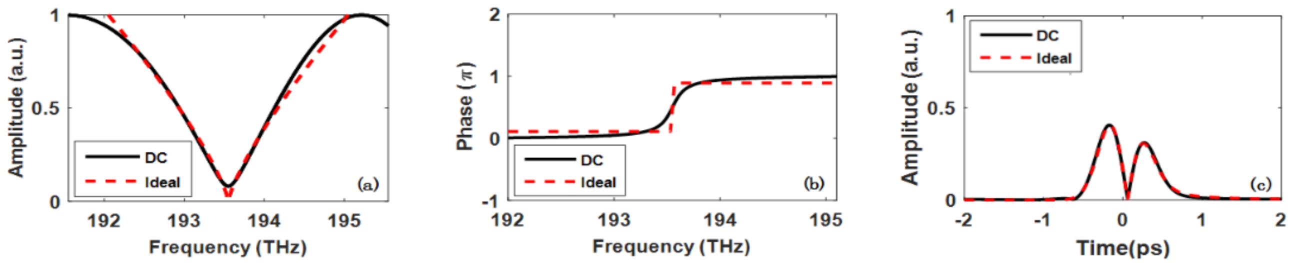


**FIGURE 5.** (a) Magnitude response and (b) phase response of the transmission spectrum of the asymmetric DCs with $a_1 = 3.7\ \mu m$, $a_2 = 3.75\ \mu m$, $d = 9\ \mu m$, $n_{core1} = 1.449$, $n_{core2} = 1.449$, $n_{clad} = 1.444$. The dashed line shows the magnitude and phase response of an ideal FOD. (c) Simulated output pulse. The dashed line shows the output pulse from an ideal FOD. The fractional order is 0.78.

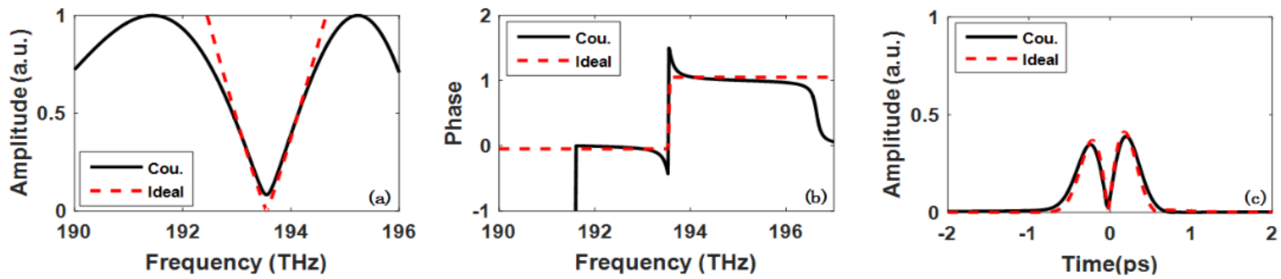


**FIGURE 6.** (a) Magnitude response and (b) phase response of the transmission spectrum of the asymmetric DCs with $a_1 = 3.75\ \mu m$, $a_2 = 3.7\ \mu m$, $d = 9\ \mu m$, $n_{core1} = 1.449$, $n_{core2} = 1.449$, $n_{clad} = 1.444$. The dashed line shows the magnitude and phase response of an ideal FOD. (c) Simulated output pulse. The dashed line shows the output pulse from an ideal FOD. The fractional order is 1.1.

of three kinds of couplers with specific structures that can be designed for FODs with orders of 0.47, 0.78, 1.1 are 0.871 *mm*, 0.897 *mm*, 0.927 *mm* at the center frequency respectively. The lengths of the couplers must be an integer multiple of the coupling lengths of the couplers. The lengths of the couplers with three specific structures are 88 *mm*, 90.8*mm*, 93.6 *mm* respectively. The device functionality is dependent on the length of the coupler. Therefore, the length of the coupler must be strictly controlled.

Through the above analysis, it is feasible to achieve FOD by finding a specific DC structure. Further, the relation between the order of the FOD and the structure parameters of the DC is analyzed. The variation of the order of the FOD with $n_{core2}$ is shown in Fig. 7(a) when the other parameters are $n_{core1} = 1.4491$, $n_{clad} = 1.444$, $a_1 = 3.9\ \mu m$, $a_2 = 3.9\ \mu m$, $d = 9\ \mu m$. The order of FOD decreases as $n_{core2}$ increases. The variation of the order of the FOD with $a_2$ is shown in Fig. 7(b) when the other parameters are $n_{core1} = 1.449$, $n_{core2} = 1.449$, $n_{clad} = 1.444$, $a_1 = 3.6\ \mu m$, $d = 9\ \mu m$. The order of the FOD decreases as $a_2$ increases. The variation of the order of FOD with $d$ is shown in Fig. 7(c) when the other parameters are $n_{core1} = 1.4491$, $n_{core2} = 1.4492$, $n_{clad} = 1.444$, $a_1 = 3.9\ \mu m$, $a_2 = 3.9\ \mu m$. The order of FOD increases firstly as $d$ increases, then the order of the FOD decreases as $d$ increases. Hence, the order of FOD can be controlled by changing the parameters of DC, which means that arbitrary order FOD could be realized through different DCs.

The processing error (D) and energetic efficiency (E) are two important parameters that characterize the performance of the differentiator, whose definitions are as follows [16], [31], [32]

$$D = \frac{\int \left| |f(t)|^2 - |g(t)|^2 \right| dt}{\int |g(t)|^2 \, dt} \tag{7}$$

$$E = \frac{\int_{-\infty}^{\infty} \left| f_{out}^2(t) \right| dt}{\int_{-\infty}^{\infty} \left| f_{in}^2(t) \right| dt} \tag{8}$$

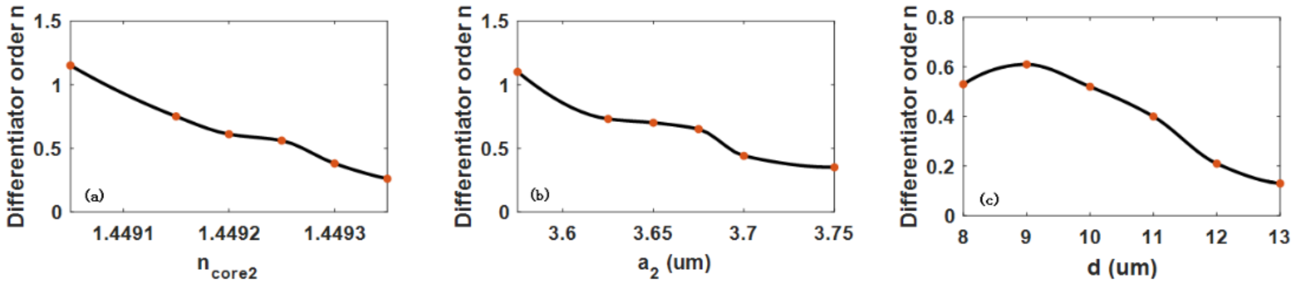


**FIGURE 7.** The FOD order varies with $n_{core2}$, $a_2$, and $d$.

where the $f(t)$ represents the output of the proposed FOD, $g(t)$ represents the output of the ideal FOD, and both signals have been normalized to unity. $f_{out}(t)$ represents the actual output signal from DC and $f_{in}(t)$ represents the actual input signal. The calculated processing errors of the three FODs with orders of 0.47, 0.78, 1.1 are 10.04%, 6.11%, 22.24 % and the energetic efficiencies are 20.61%, 19.62%, 20.39% respectively.

The processing error of the proposed FOD firstly decreases when the FWHM of the input pulse increases as Fig. 8 shows. This is because the input pulse with smaller FWHM has a larger bandwidth, which may be larger than the device-operation bandwidth of the FOD. Then the processing error increases as Fig. 8 shows, because the magnitude of the FOD has deviated from the magnitude of the ideal FOD at the central wavelength. The proposed FOD has an operation bandwidth of a few terahertz and a high energetic efficiency.

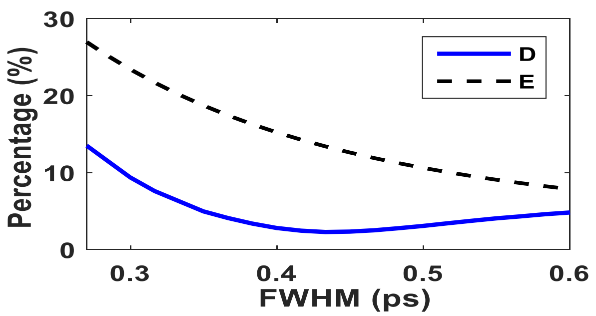


**FIGURE 8.** The processing error (D) and energetic efficiency (E) of the FOD achieved by using asymmetric DC with $a_1 = 3.6\ \mu m$, $a_2 = 3.7\ \mu m$, $d = 9\ \mu m$, $n_{core1} = 1.449$, $n_{core2} = 1.449$, $n_{clad} = 1.444$ with different FWHM of the input pulse.

## IV. CONCLUSION

In summary, the fractional-order differentiator based on the asymmetric wavelength-selective DC is proposed and demonstrated. The order of the optical differentiator is determined by the structural parameters of the asymmetric wavelength-selective DC, i.e., the coupling coefficient and the propagation constant difference of the two waveguides of the coupler. The relation between the order of the FOD and the structure parameters of the DC is analyzed and discussed. When the pulse is launched into the waveguide with a smaller propagation constant, the order of the FOD is smaller than 1. When the pulse is launched into the waveguide with a bigger propagation constant, the order of the FOD is larger than 1. Three sets of asymmetric wavelength-selective DCs are designed to implement the FODs with orders of 0.47, 0.78, and 1.1, whose processing errors are 10.04%, 6.11%, 22.24% and energetic efficiencies are 20.61%, 19.62%, 20.39% respectively. The proposed FOD has a large operation bandwidth and simple structure, which provides a feasible and competitive way for the design and implement of FODs.

## REFERENCES

[1] J. Azaña, "Ultrafast analog all-optical signal processors based on fiber-grating devices," *IEEE Photon. J.*, vol. 2, no. 3, pp. 359–386, Jun. 2010.
[2] M. Liu *et al.*, "Widely tunable fractional-order photonic differentiator using a Mach–Zenhder interferometer coupled microring resonator," *Opt. Express*, vol. 25, no. 26, pp. 33305–33314, Dec. 2017.
[3] X. Liu and X. Shu, "Design of an all-optical fractional-order differentiator with terahertz bandwidth based on a fiber Bragg grating in transmission," *Appl. Opt.*, vol. 56, no. 24, pp. 6714–6719, Aug. 2017.
[4] T. Wu, C. Zhang, H. Zhou, H. Huang, and K. Qiu, "Photonic microwave waveforms generation based on frequency and time-domain synthesis," *IEEE Access*, vol. 6, pp. 34372–34379, 2018.
[5] T.-J. Ahn and J. Azaña, "Wavelength-selective directional couplers as ultrafast optical differentiators," *Opt. Express*, vol. 19, no. 8, pp. 7625–7632, Jul. 2011.
[6] Y. Park, M. Kulishov, R. Slavík, and J. Azaña, "Picosecond and sub-picosecond flat-top pulse generation using uniform long-period fiber gratings," *Opt. Express*, vol. 14, no. 26, pp. 12670–12678, Dec. 2006.
[7] C. Cuadrado-Laborde, "All-optical ultrafast fractional differentiator," *Opt. Quantum Electron.*, vol. 40, no. 13, pp. 983–990, Mar. 2008.
[8] F. Li, Y. Park, and J. Azaña, "Complete temporal pulse characterization based on phase reconstruction using optical ultrafast differentiation (PROUD)," *Opt. Lett.*, vol. 32, no. 22, pp. 3364–3366, Nov. 2007.
[9] F. Liu *et al.*, "Compact optical temporal differentiator based on silicon microring resonator," *Opt. Express*, vol. 16, no. 20, pp. 15880–15886, 2008.
[10] J. Dong *et al.*, "High-order photonic differentiator employing on-chip cascaded microring resonators," *Opt. Lett.*, vol. 38, no. 5, pp. 628–630, Mar. 2013.
[11] Y. Park, R. Slavík, and J. Azaña, "Ultrafast all-optical first- and higher-order differentiators based on interferometers," *Opt. Lett.*, vol. 32, no. 6, pp. 710–712, Mar. 2007.
[12] J. Xu, X. Zhang, J. Dong, D. Liu, and D. Huang, "High-speed all-optical differentiator based on a semiconductor optical amplifier and an optical filter," *Opt. Lett.*, vol. 32, no. 13, pp. 1872–1874, Jul. 2007.
[13] N. K. Berger, B. Levit, B. Fischer, M. Kulishov, D. V. Plant, and J. Azaña, "Temporal differentiation of optical signals using a phase-shifted fiber Bragg grating," *Opt. Express*, vol. 15, no. 2, pp. 371–381, Jan. 2007.
[14] M. Kulishov and J. Azaña, "Design of high-order all-optical temporal differentiators based on multiple-phase-shifted fiber Bragg gratings," *Opt. Express*, vol. 15, no. 10, pp. 6152–6166, Feb. 2007.

[15] X. Liu, X. Shu, and H. Cao, "Proposal of a phase-shift fiber Bragg grating as an optical differentiator and an optical integrator simultaneously," *IEEE Photon. J.*, vol. 10, no. 3, Jun. 2018, Art. no. 7800907.
[16] M. Kulishov and J. Azaña, "Long-period fiber gratings as ultrafast optical differentiators," *Opt. Lett.*, vol. 30, no. 20, pp. 2700–2702, Oct. 2005.
[17] R. Slavík, Y. Park, M. Kulishov, R. Morandotti, and J. Azaña, "Ultrafast all-optical differentiators," *Opt. Express*, vol. 14, no. 22, pp. 10699–10707, Oct. 2006.
[18] X. Liu and X. Shu, "Design of arbitrary-order photonic temporal differentiators based on phase-modulated fiber Bragg gratings in transmission," *J. Lightw. Technol.*, vol. 35, no. 14, pp. 2926–2932, Jul. 15, 2017.
[19] P. Melchior, M. Cugnet, J. Sabatier, A. Poty, and A. Oustaloup, "Flatness control of a fractional thermal system," in *Proc. 2nd Symp. Fractional Derivatives Appl. (FDTAs)*, Long Beach, CA, USA, 2007, pp. 493–509.
[20] M. Li, L.-Y. Shao, J. Albert, and J. Yao, "Continuously tunable photonic fractional temporal differentiator based on a tilted fiber Bragg grating," *IEEE Photon. Technol. Lett.*, vol. 23, no. 4, pp. 251–253, Feb. 15, 2011.
[21] H. Shahoei, J. Albert, and J. Yao, "Tunable fractional order temporal differentiator by optically pumping a tilted fiber Bragg grating," *IEEE Photon. Technol. Lett.*, vol. 24, no. 9, pp. 730–732, May 1, 2012.
[22] A. Zheng, T. Yang, X. Xiao, Q. Yang, X. Zhang, and J. Dong, "Tunable fractional-order differentiator using an electrically tuned silicon-on-isolator Mach–Zehnder interferometer," *Opt. Express*, vol. 22, no. 15, pp. 18232–18237, Jul. 2014.
[23] A. Zheng *et al.*, "Fractional-order photonic differentiator using an on-chip microring resonator," *Opt. Lett.*, vol. 39, no. 21, pp. 6355–6358, Nov. 2014.
[24] C. Cuadrado-Laborde and M. V. Andrés, "In-fiber all-optical fractional differentiator," *Opt. Lett.*, vol. 34, no. 6, pp. 833–835, Mar. 2009.
[25] G. P. Agrawal, *Applications of Nonlinear Fiber Optics*. San Diego, CA, USA: Academic, 2001, pp. 74–75.
[26] W. Zhang, W. Liu, W. Li, H. Shahoe, and J. Yao, "Independently tunable multichannel fractional-order temporal differentiator based on a silicon-photonic symmetric Mach–Zehnder interferometer incorporating cascaded microring resonators," *J. Lightw. Technol.*, vol. 33, no. 2, pp. 361–367, Jan. 15, 2015.
[27] S. Zheng, G. Ren, Z. Lin, and S. Jian, "Mode-coupling analysis and trench design for large-mode-area low-cross-talk multicore fiber," *Appl. Opt.*, vol. 52, no. 19, pp. 4541–4548, Jul. 2013.
[28] M. Li, H.-S. Jeong, J. Azaña, and T.-J. Ahn, "25-terahertz-bandwidth all-optical temporal differentiator," *Opt. Express*, vol. 20, no. 27, pp. 28273–28280, 2012.
[29] T. L. Huang, A. L. Zheng, J. J. Dong, D. S. Gao, and X. L. Zhang, "Terahertz-bandwidth photonic temporal differentiator based on a silicon-on-isolator directional coupler," *Opt. Lett.*, vol. 40, no. 23, pp. 5614–5617, Dec. 2015.
[30] H.-S. Jeong, C.-Y. Kim, W. Shin, and T.-J. Ahn, "Dual-wavelength first-order optical differentiators based on bidirectional fiber couplers," *J. Opt.*, vol. 15, Apr. 2013, Art. no. 055405.
[31] H. You *et al.*, "Optical temporal differentiator using a twin-core fiber," *Opt. Eng.*, vol. 52, no. 1, Jan. 2013, Art. no. 015005.
[32] H. You, T. Ning, J. Li, W. Jian, X. Wen, and L. Pei, "Design and performance analysis of high-order optical temporal differentiator with twin-core fiber," *Opt. Eng.*, vol. 52, no. 8, Aug. 2013, Art. no. 086101.

**TING-TING YAN** received the bachelor's degree from Henan Normal University, in 2016. She is currently pursuing the master's degree with Beijing Jiaotong University. Her research interests include optical device and optical signal processing.

**WEN-HUA REN** received the bachelor's and Ph.D. degrees from Beijing Jiaotong University, China, in 2005 and 2010, respectively, where he is currently an Associate Professor with the Institute of Lightwave Technology. His research interests include special optical fiber and optical fiber lasers.

**YOU-CHAO JIANG** received the bachelor's and Ph.D. degrees from Beijing Jiaotong University, China, in 2013 and 2018, respectively, where he is currently a Lecturer with the Institute of Lightwave Technology. His research interests include special optical fiber, orbital angular momentum, and optical fiber lasers.